SAN FRANCISCO ESTUARY & WATERSHED SCIENCE
Sponsored by the Delta Stewardship Council and UC Davis Institute of the Environment

RESEARCH

Predicting Sediment Bulk Density for San Francisco Estuary

Samantha C. McGill [1], Jessica R. Lacy [1]

ABSTRACT

Sediment bulk density (ρ_{dry}) and particle size are two important parameters for predicting sediment bed erosion. ρ_{dry}, however, is difficult to measure accurately. The units of ρ_{dry} have not been consistently reported in the literature, leading to confusion, particularly in the calculation of sediment budgets that typically require integrating mass-based and volumetric components. Relationships between ρ_{dry} and sediment composition have been developed for multiple regions and differ between systems. Developing a system-specific predictive model for ρ_{dry} can help fill data gaps and improve sediment budgets, model accuracy, and estimates of quantities of sediment needed for restoration. In this study, we investigate whether ρ_{dry} in San Francisco Estuary can be predicted from organic carbon content or percent of fines, which are more easily or frequently measured than ρ_{dry}. We compiled sediment properties from samples collected over the past decade throughout the intertidal and subtidal regions of San Francisco Bay and the Sacramento–San Joaquin Delta to examine this relationship. Sample composition ranged from 2.18 to 99.97% fines (particles <0.0625 mm), ρ_{dry} ranged from 0.22 to 1.60 g cm^{-3}, and organic carbon ranged from 0.06 to 7.98%. Regression analysis indicates that the percent of fines explains 93% of the variation of ρ_{dry} (p-value <0.05, $N=81$). The coefficient of determination decreased by ~1% when organic carbon was incorporated in the regression analysis. Comparison of this predictive ρ_{dry} model to four published models based on samples from other regions supports previous findings that the relationship between ρ_{dry} and particle size may vary by system. We also examined additional factors that may affect sediment erodibility, such as hydrographic and oceanographic conditions. Classification of sample sites as intertidal vs. subtidal or wavy vs. non-wavy each significantly explained the residuals from the ρ_{dry} model, and both intertidal and wavy conditions were associated with higher ρ_{dry} values.

SFEWS Volume 23 | Issue 4 | Article 6

https://doi.org/10.15447/sfews.2025v23iss4art6

* Corresponding author: scmcgill@usgs.gov

1 US Geological Survey
Pacific Coastal and Marine Science Center
Santa Cruz, CA 95060 USA

KEY WORDS

dry bulk density, particle size, sediment organic carbon, estuarine sediments, San Francisco Bay, Sacramento–San Joaquin Delta

INTRODUCTION

Sediment is a valuable resource that is increasingly in demand, particularly in San Francisco Estuary (the estuary) where there are multiple uses for it. Sediment is needed in the estuary to support vertical accretion of wetlands to counter local subsidence and keep pace with sea level rise, as well as for restoration projects that typically involve converting subsided salt ponds and agricultural tracts back to wetlands. At the same time, sediment supply to the estuary has declined during recent decades (Wright and Schoellhamer 2004).

The development of sediment budgets, which are utilized for restoration planning and modeling, typically requires conversions between mass-based and volume-based measures of sediment. This conversion depends on the bulk density of the sediment. An inaccurate bulk density value can have a sizable consequence. For example, a sensitivity analysis by Brew and Williams (2010) tested a range of values and assumptions for different components used in their sediment budget calculation to see how they would influence mudflat change over 50 years. The calculated total mudflat area decreased 10% from 26 to 23 km^2 when they increased their estimate of bulk density for deposited sediment by about 15%, from 1.3 to 1.5 g cm^{-3}. The result of this change was comparable to decreasing estuarine sediment input from a long-term average down to 0.

Another important application of bulk density is quantification of carbon sequestration rates where sediment dry bulk density (ρ_{dry}) is used along with the carbon content of sediments to calculate the carbon density (Ezcurra 2024). Bulk density is also considered a predictor of sediment erodibility and a required input for sediment transport models (Allen et al. 2021) that has been shown to affect benthic organisms; lower bulk densities promote bioturbation and faster burrowing among benthic macrofauna (Weisebron et al. 2021).

Sediment bulk density is a physical property of the bed that tells us how compacted particles of sediment are within a specified volume. It is reported either as a wet (aka saturated) bulk density, which represents the combined sediment and water mass per unit volume, or as dry bulk density (ρ_{dry}), which is the dry sediment mass per unit volume. Dry bulk density can be measured two ways: (1) by collecting a sample of a known volume, then obtaining the dry weights or (2) by obtaining the wet and dry weights of a sample, and assuming a sediment particle density (often quartz 2.65 g cm^{-3}) and a pore water density. Some studies account for the salt mass that is left behind when the pore water is evaporated during the drying process. An additional correction for organic content can be made for sediments from marshes or other regions with high levels of organics. Bulk density is challenging to measure and inconsistently reported because of the range of protocols that have been used. Flemming and Delafontaine (2000) point out the confusion surrounding bulk density content and concentration, highlighting its misuse in multiple studies. Similar problems occur in the estuary. The San Francisco Estuary Institute compiled bulk density data from the estuary and reported finding several sources of confusion, including terminology, units, wet vs. dry, organic vs. mineral or inorganic, and application of values from inappropriate periods and systems (McKnight et al. 2020).

Particle size has a long history of use in sediment transport studies and is not associated with the same confusion and inconsistencies as bulk density. Particle size has been measured throughout San Francisco Bay (Barnard et al. 2013). Although there are some variations among protocols for measuring particle size, samples tend to be handled and results reported similarly across studies. With a growing interest in blue carbon—carbon captured and stored in ocean and coastal ecosystems (Mcleod et al. 2011)—measurements of sediment organic carbon content are becoming more common. Organic carbon content is typically inversely related to bulk density (Avnimelech et al. 2001). An expression that predicts bulk density from particle size and/or organic carbon would substantially increase the spatial extent of the estuary for which bulk density can be estimated.

Throughout this paper, we focus on sediment dry bulk density (ρ_{dry}): the term "bulk density" always refers to sediment dry bulk density. We use percent of fines (P_{fines}) as the measurement of particle size. This study focuses on properties of the top 1 cm of the sediment bed (estuary floor). This surficial layer of the sediment bed is most influenced by bed shear stress from waves and currents, and is most relevant to sediment transport processes and modeling. In the estuary, the depth of erosion during wave events is typically on the order of 1 cm (Brand et al. 2010; Egan et al. 2020).

The goals of this study are to: (1) provide an overview of the spatial variability of bulk density throughout the estuary, including the Sacramento–San Joaquin Delta (the Delta); (2) determine whether particle size and organic carbon content are useful predictors of bulk density for the estuary, and compare results to models currently in the literature; and (3) explore other environmental factors that may influence bulk density.

BACKGROUND

In the literature, several predictive models demonstrate the relationship between sediment properties and bulk density. Many of these models are based on sediments from a specific region; none of them claim to be universally applicable. To our knowledge, there are no models based on sediment from the estuary. Besides being site-specific, several of the existing models are dated and are not published in open-access journals. We selected four of the most used, more recent, and accessible models to compare to our data and model.

Flemming and Delafontaine (2000) present a relationship between mud content (dry weight %) and dry bulk density (g cm^{-3}) for samples collected along sand–mud gradients in the East Frisian Wadden Sea (Equation 1; East Frisian Wadden Sea–Flemming: EFWS–F). Flemming and Delafontaine point out that the relationship between ρ_{dry} and mud content varied for different geographic regions, but that all regions can use an equation of the same form (Equation 2; General Form–Flemming: GF–F). Mud content used by Flemming and Delafontaine (2000) is the same quantity that we refer to as percent fines (P_{fines}).

$$\rho_{dry} = -0.7955892 + 2.3863045^{\left(\frac{-mud\ content}{125.8292772}\right)} \quad \text{Eq 1}$$

$$\rho_{dry} = a + b * exp^{\frac{-mud\ content}{c}} \quad \text{Eq 2}$$

Van Rijn and Barth (2018) developed a relationship between dry bulk density and sediment composition for samples collected from a tidal channel of Noordpolderzijl, on the edges of the Wadden Sea. Their model incorporates the effects of different size classes (clay, silt, and sand) as well as the effects of organics (Equation 3). The model is based on data from both field and laboratory experiments, in which some of the sediments were exposed to a short-term consolidation period on the order of weeks to months. Clay is defined as particles smaller than 0.0039 mm, silt comprises particles between 0.0039 mm and 0.0625, sand is particles between 0.625 and 2 mm (Wentworth 1922).

$$\rho_{dry} = \left(1 - \frac{P_{org}}{100}\right)\left[400\left(\frac{P_{clay}}{100}\right) + 800\left(\frac{P_{silt}}{100}\right) + 1600\left(\frac{P_{sand}}{100}\right)\right] \quad \text{Eq 3}$$

where P_{org}, P_{clay}, P_{silt}, and P_{sand} are percent by weight of organics, clay, silt, and sand, respectively.

Mulder (1995) as cited by Alonso et al. (2021), used unconsolidated sediments from the Ems Estuary, which also connects to the Wadden Sea, to develop a model of dry bulk density based on percent of sand (Equation 4):

$$\rho_{dry} = 450 + 4.5 * P_{sand} + 0.063 * {P_{sand}}^2 \quad \text{Eq 4}$$

METHODS

Sampling Location and Collection

Sediment property data were compiled from several studies that took place in and around San Francisco Bay (the bay) and the Sacramento–San Joaquin Delta (the Delta) between August 2014 and April 2024. A total of 81 temporally or spatially distinct samples were analyzed: 52 of the samples were from the bay and 29 from the

https://doi.org/10.15447/sfews.2025v23iss4art6

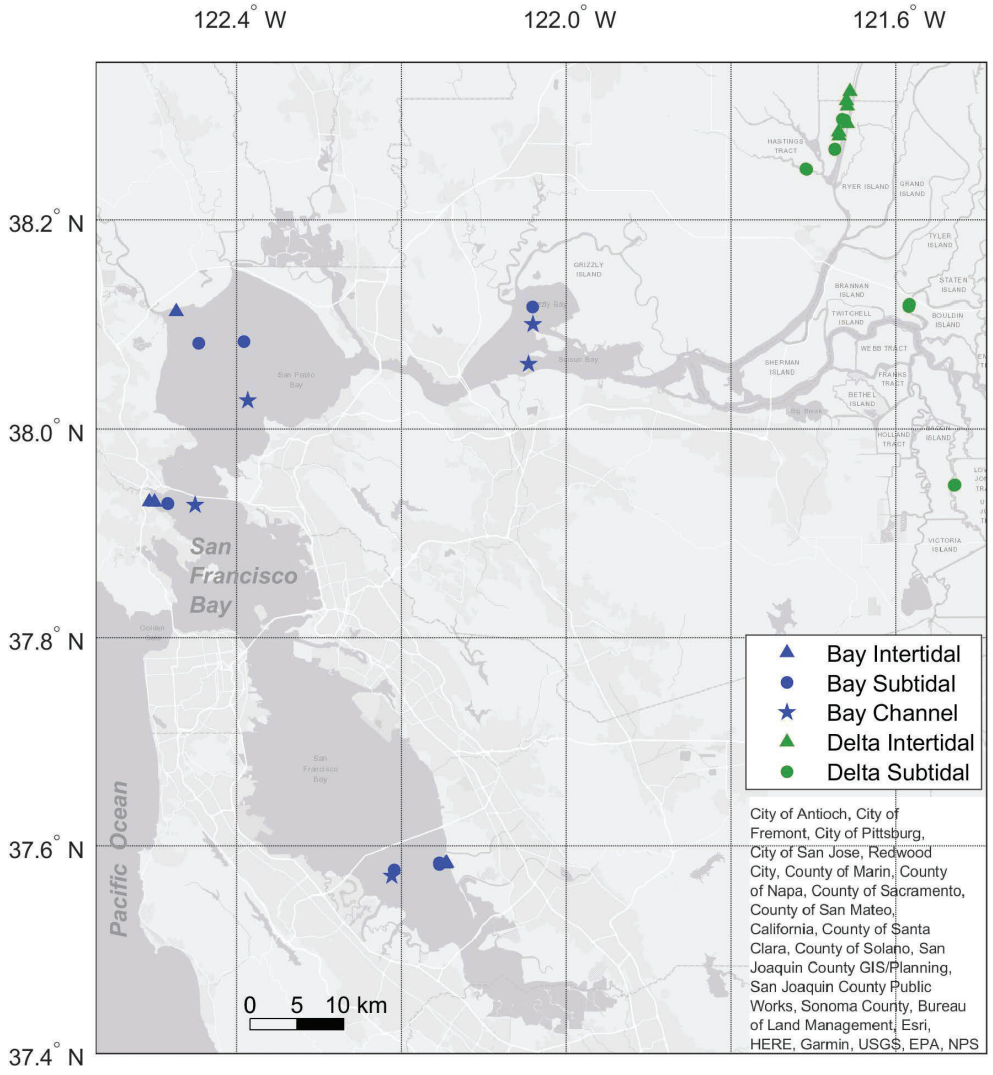

Figure 1 Map showing locations of cores coded by tidal regime and colored by region within the San Francisco Estuary

Delta (Figure 1). The goals of the studies differed; therefore, some sites were sampled only once, while others were sampled repeatedly over time, and replicates were collected at some sites but not others.

Sites in the Delta included tidally influenced channels and shallows in restored former agricultural tracts. Bay sites included subtidal and intertidal shallows in Grizzly Bay, San Pablo Bay, Corte Madera Bay, and the region of San Francisco Bay that extends below the Bay Bridge (South Bay), channels of Suisun, San Pablo, and South bays, as well as a tidal creek within Muzzi Marsh. Details on the sampling sites and datasets used are shown in Table 1.

We collected all samples with push cores, either by hand push core, pole-mounted push core (varying diameter), or by Gomex box core that was subsampled using smaller push cores (3.7 cm). Cores were capped with water-tight lids until transported back to shore where sectioning took place. The cores were sectioned in 0.5- or 1-cm vertical increments and placed in pre-weighed Whirl-Pak bags. Samples were kept in cold storage until ready for processing by the US Geological Survey (USGS) Sediment Laboratory in Santa Cruz, California. The laboratory analyzed

Table 1 Summary of datasets with the range of sample collection dates, region and location of collection, number of samples for each sub-region and data source. Citations for the data sources are provided in the final column based on the different types of data used: sediment (Sed), bathymetric (Bathy), and hydrodynamic (Hydro).

Region	Site	Site description	Number of samples	Date collected	Data release sources
Central Delta	Mokelumne River	tidal channel	3	3/14/2018	Sed/Bathy/Hydro: Lacy et al. (2020)
South Delta	Middle River	tidal channel	3	3/19/2018	
North Delta	Lindsey Slough	backwater	2	4/4/2017	
North Delta	Liberty Island	intertidal and subtidal (former agriculture tract)	10	8/25/2014–8/20/2019	Sed: Lacy et al. (2018) Hydro: Lacy et al. (2016) Bathy: Snyder et al. (2016b)
North Delta	Little Holland Tract	intertidal and subtidal (former agriculture tract)	11	8/26/2014–8/20/2019	
North Bay	Grizzly Bay	subtidal and channel	16	6/13/2019–4/25/2024	Sed/Hydro:(Lacy et al. (2020) Sed/Hydro: McGill et al. (2021) Sed: McGill, Lacy, Tan (2025)
North Bay	San Pablo Bay	intertidal, subtidal, and channel	20	6/12/2019–4/25/2024	Sed/Hydro: Lacy et al. (2020) Sed/Hydro: McGill et al. (2021) Sed/Hydro: McGill et al. (2024) Sed: McGill, Lacy, Tan (2025)
Central Bay	Corte Madera Bay	tidal creek, intertidal, subtidal and channel	7	4/12/2022–4/25/2024	Sed/Hydro: (McGill et al. 2024) Sed: (McGill, Lacy, Tan 2025)
South Bay	South Bay	intertidal, subtidal, and channel	8	6/4/2021–3/5/2024	Sed: Ferreira et al. (2023) Hydro: Ferreira et al. (2023) Sed: McGill, Lacy, Tan (2025) Sed/Hydro: McGill, Lacy, Stevens, et al. (2025)
North Bay	Suisun Bay	near channel	1	4/25/2024	Sed: McGill, Lacy, Tan (2025)

the samples for bulk density, particle size, and total organic carbon content, as detailed below. Results for 0.5-cm vertical core sections were averaged together to represent the top 1 cm. Replicate sediment cores were averaged together as well.

Sample Analysis

Bulk Density

Soon after sectioning, the initial "wet" weights of the samples were measured in the laboratory. Once weighed, samples were placed in a 60 °C oven until fully dried, and were then placed in a desiccator for an hour before dry weights were measured. The samples were then placed back in the oven for another 4 hours at 60 °C, moved to the desiccator for 1 hour, and re-weighed. This process was repeated until their weights were equal to or varied less than 0.5% from their previously recorded dry weight.

We applied a correction for salt mass following Dadey et al. (1992). The mass of salt in each sample was determined based on the local salinity (parts per thousand, ppt) measured by instruments near the sampling site and subtracted from the sample's dry sediment mass. Bulk density was calculated as follows:

$$porosity = \frac{\left(\frac{m_w}{\rho_w}\right)}{\left(\frac{m_s}{\rho_s} + \frac{m_w}{\rho_w}\right)} \quad \text{Eq 5}$$

$$\rho_{dry} = (1 - porosity) * \rho_s \quad \text{Eq 6}$$

where m_s = mass of dry sediment (salt corrected); m_w is the mass of water; ρ_s is the density of sediment, assumed to be 2.65 g cm^{-3}; and ρ_w is the density of water, assumed to be 1 g cm^{-3}.

We performed a check between the density-based method we used and a commonly used

https://doi.org/10.15447/sfews.2025v23iss4art6

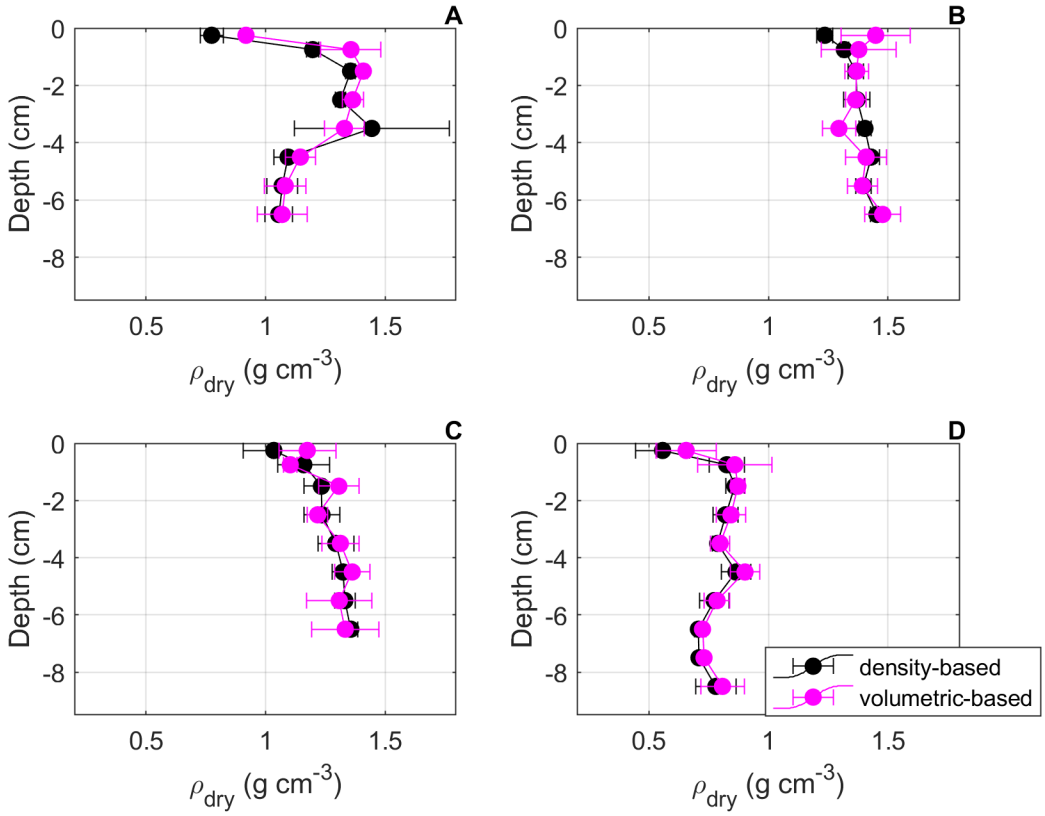

Figure 2 Profiles of bulk density for four sites in South San Francisco Bay. Mean and standard deviation of bulk density from three replicates at each site from the density-based method (*black*) and the volumetric-based method (*magenta*).

volumetric method. To calculate bulk density using the volumetric method, we divided the dried sediment weight by the volume of the core section sampled, which was calculated from the measured core diameter and the section thickness (Flemming and Delafontaine 2000). A comparison of several cores showed no significant difference in dry bulk density using the two methods for non-surface core sections (Figure 2). The surface of the cores can be sloped or may have uneven features and textures, making it hard to get the exact thickness, which introduces error in the volumetric method. Sections from further down core tend to retain a more complete cylindrical shape when sampled, providing a better comparison between bulk density methods. The bulk density data presented in this paper were calculated using the density-based method, which we expect to be more accurate for irregular surface sections.

Particle Size

Subsamples were collected and prepared for particle size analysis by treating them with hydrogen peroxide to remove organics then heating them to remove excess hydrogen peroxide. Next, samples were placed in an ultrasonic bath to disperse silt and clay from sand and larger-sized particles and were rinsed with deionized water and centrifuged to remove soluble ions. Subsequently, the samples were wet sieved with 1-mm and 0.0625-mm sieves to segregate the combined gravel and coarse sand fraction (>1 mm), sand (1 mm to 0.0625 mm), and mud (<0.0625 mm). Samples collected during and after 2021 had shells greater than 1 mm removed and weighed during the sieving process. The sand and coarser-size fractions were dry sieved and weighed. The mud fraction was treated with a dispersant, dried, and weighed. The mud and sand fractions were separately analyzed using a Beckman Coulter LS 13 320. For this study, we

examined particle size by using fines (P_{fines}), which represents the percent of sample that is smaller than 0.0625 mm.

Carbon

Total organic carbon content (P_{OC}), expressed in units of percent weight, was determined using techniques described in McGill et al. (2024). In short, this process involved measuring the total carbon content through combustion, and total inorganic carbon content through acid digestion, then calculating total organic carbon as the difference between the two. The mean and median organic carbon content of samples from this study were 1.38% and 1.31%, respectively, and all but one sample were less than 3% organic carbon. Therefore, because of the very low percentage of organics present in this dataset, the bulk density values were not corrected for the organic component.

Additional Analyses and Corrections

Some of the samples collected from South Bay had higher shell concentrations than other sites. The bulk density method we used assumes particles have a density equal to that of quartz, so we determined shell density to assess the error introduced by a significant shell fraction. Shells >1 mm were removed from subsamples for particle size analysis. These shell fragments were weighed to determine percent shell by mass of the subsample. Shell mass for the subsamples of individual core sections (before averaging the top two sections and replicates together) ranged from 0% up to 25.17%, with a median of 1.91%. Sixty-one of the 144 sections analyzed for percent shell had >1% shell, while only 17 sections were 10% or more shell. In an effort to gather more shell, the remaining sample of five to six sections from three sites with the highest calcium carbonate contents (P_{CaCO3}) were combined, resulting in a single sample per site. The shells were cleaned using hydrogen peroxide, boiled, sonicated, and sieved using a 1-mm mesh. The masses and volumes of shell from the three sites were obtained using a balance and displacement of water in a graduated cylinder, and used to calculate shell density. The mean of the three shell densities was 2.852 g cm^{-3} (standard deviation: 0.4115 g cm^{-3}), quite similar to the density of quartz (2.65 g cm^{-3}). Shell-corrected bulk density was calculated using mean shell density for the shell fraction of the sample. The corrected bulk densities were not significantly different from the original bulk density values (Figure 3A). Since bulk densities for samples that

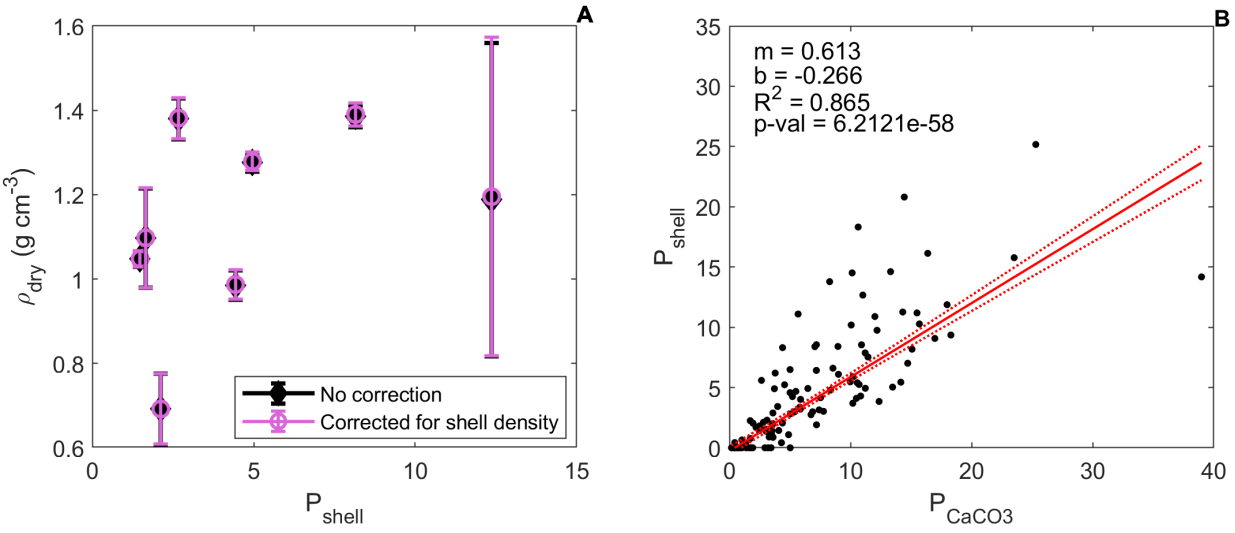

Figure 3 (**A**) Mean and standard deviation of top 1-cm replicates of uncorrected bulk density (*black*) and shell-density corrected bulk density (*magenta*), plotted against shell content. (**B**) Shell content vs. calcium carbonate content for South Bay core sections: data and regression line (*red solid*), with slope (m), intercept (b), coefficient of determination (R^2), and the *p*-value. Above and below the regression line are 95% confidence bounds on the regression.

https://doi.org/10.15447/sfews.2025v23iss4art6

had the greatest shell content did not change significantly when corrected for shell density, we proceeded to use our original uncorrected bulk density values for all of the samples.

We also tested how well calcium carbonate content predicts shell content. We used all of the samples available from South Bay that were analyzed for calcium carbonate and shell; similar to the shell density analysis, these samples represented individual core sections.

Methods of Analysis

Regression Analysis

We used an iteratively re-weighted least-squares (IRLS) linear regression to examine the relationship between the different sediment properties. IRLS differs from the commonly used ordinary least-squares (OLS) fitting method by including a weight as an additional scale factor during the fitting process. IRLS does not rely as heavily upon meeting OLS assumptions (Hoaglin et al. 1985). We used both linear regression as well as multiple regression to examine our dataset; therefore, we focus on the adjusted coefficients of determination. However, we report the ordinary coefficients of determination in table format.

We applied IRLS to three datasets based on region within the estuary. One dataset, "Bay samples," exclusively comprised samples collected within San Francisco Bay, which includes South Bay up through Grizzly and Suisun bays. Another dataset, "Delta samples," contained only samples from the Delta. The final dataset tested was a combination of both the Bay and Delta samples, which we refer to as "All samples."

Kruskal–Wallis Tests for Environmental Influence

We used Kruskal–Wallis (KW) tests (Kruskal and Wallis 1952) to see if various environmental factors explained the residuals from the bulk density model. The KW test is a non-parametric alternative to the one-way analysis of variance (ANOVA) test, and does not require that the data follow a statistical distribution. The KW test investigates if a statistically significant difference between the medians of two or more independent groups exists. We chose environmental factors known to potentially affect bulk density or sediment erodibility, and classified the samples for each factor as follows:

Tidal Regime. Each sample was classified as being either in a subtidal or intertidal environment. Sites that had an elevation below 0 MLLW were considered subtidal, while those above 0 MLLW were considered intertidal. Samples from bay channels were all classified as subtidal. Samples from certain stations in the Delta were classified based on information from literature (Snyder et al. 2016a; Lacy et al. 2021, 2023). Most of the samples were collected at or near stations where hydrodynamic parameters were collected. These stations also tended to have survey grade elevation data or elevation derived from bathymetric data available; these datasets can be found in Table 1. When hydrodynamic data were unavailable, water-level data from the closest USGS gage (USGS 2024; ID: 11455140, 11455276) were used.

Drought. Drought indices were obtained from the US Drought Monitor's Drought Severity and Coverage Index (DSCI) (Akyuz 2017). DSCI data were collected for the Sacramento area to capture freshwater input through the Sacramento–San Joaquin Delta. DSCI ranged from 0 to 500, and were binned into two groups: no to low drought (< 100 DSCI) and elevated drought conditions (> 100 DSCI).

Waviness. Samples from the Mokelumne River, Middle River, and bay channels were classified as non-wavy because the short-period wind waves occurring in the estuary do not reach the bed at these deeper stations. For all other sites, we utilized wave data collected nearby for the classification (Table 1) or referred to the literature (Lacy et al. 2023). We determined the percent of time that significant wave height (H_{sig}) exceeded 0.1 m for a period representative of the wave climate at each site around the time of sampling. For most samples, the period spanned about a month before the sediment sample collection date. If data were not available for that period, we used the 15 days after the sediment sample was

collected. Sample periods with significant wave heights exceeding 0.1 m more than 50% of the time were classified as wavy.

Energy. The energy categorization indicates the effect of waves or currents. Within the bay, the range of tidal velocities is greater in the channels than the subtidal and intertidal flats because RMS current speed is directly correlated with water depth (Walters et al. 1985). Bay channel sites were classified as "strong currents." In the Delta, tidal currents are weaker than in the bay, but currents can be strong during periods of high river discharge. To capture the effect of high flows, we obtained discharge data from four USGS gages (ID: 11455315, 11453000, 1131267, 11336930; USGS 2024) located within the Delta. Average discharge for the month leading up to the date samples were collected was categorized as high or low flow where high flow (and strong currents) included average discharges above 200 $m^3 s^{-1}$. The "energetic" category included all sites classified as wavy or having strong currents.

Dry and Wet Seasons. The San Francisco Estuary region has a Mediterranean climate where winters are often cool and wet, while summers are warm and dry (Conomos et al. 1985). Here we define winter or "wet season" as November through April, and summer or "dry season" as May through October. Cores were assigned to dry or wet classes based on when they were collected. The distinct seasonal pattern could play a role in sediment bulk density, since freshwater input from rainfall and snowmelt are greatest during the winter months. Wind (and thus wave) patterns also shift between seasons: during the summer, strong westerly winds develop during the afternoon, while wintertime tends to have long calm periods broken up by strong winter storms with winds from the southeast and east (Conomos et al. 1985).

Spring–Neap Tidal Cycle. Spring–neap tidal variation influences the concentration of suspended sediment in the estuary (Schoellhamer 1996) and therefore could also influence bulk density. Because the astronomical variation of tides does not vary across the estuary, we used water level highs and lows from one station to determine a spring–neap index: the NOAA Richmond station (ID: 9414863; NOAA 2024). We classified tidal energy as spring or neap for each sample, depending on whether the tidal range of the largest of the two semi-diurnal tides before sampling was greater or less than the median tidal range.

Salinity. Salinity at the time of core collection was obtained from either a deployed sensor (Table 1) or closest USGS gage data (IDs: 380631122032201, 11455780, 11455820, 375607122264701, 11162765 ; USGS 2024). When salinity data were unavailable, specific conductance was used to obtain an approximate salinity value. Sites less than two parts per thousand (ppt) were considered "fresh" while those greater than or equal to were considered saline.

Comparison of Models

We compared the performance of our model to the four models from the literature described in Equations 1 through 4. We then evaluated the models by calculating the root mean square error (RMSE) between predicted and observed dry bulk density for each model. The RMSE indicates how well a regression model fits a dataset; a lower RMSE indicates a better-fitting model.

We calculated organic matter content (P_{org}), which is required for the Van Rijn model, based on the relationship between organic carbon content (P_{OC} units: %) and organic matter content (units: %) derived from loss-on-ignition (LOI; $R^2 = 0.993$), reported for San Francisco Bay (Callaway et al. 2012).

$$P_{org} = \frac{-0.3839 \pm \sqrt{0.147378 + 0.004868 * P_{oc}}}{0.002434} \quad \text{Eq 7}$$

https://doi.org/10.15447/sfews.2025v23iss4art6

RESULTS

Sediment Properties

The sediment samples were predominantly fine (particles <0.0625 mm), with an average of 78.89% (Table 2), and a range of 2.18 to 99.97% fine. Bulk densities ranged from 0.217 to 1.60 g cm^{-3}, with an average of 0.690 g cm^{-3} (Table 2). In cores from the bay, bulk density tended to be lowest near the surface and gradually increase with depth over 2 to 6 cm (Figure 4). Samples were low in organic carbon, with a range of 0.057 to 7.98% (average 1.38%). Organic carbon was similar between Bay samples and Delta samples, and on average was higher in the Delta than the bay. However, one of the bay sites contained the highest amount of organic carbon (7.98%). On average, Bay samples tended to be slightly finer and have lower bulk densities than the Delta samples. Overall, none of the sediment properties examined were significantly different between the bay and the Delta.

Bulk Density Model

The linear regression model that most accurately predicted bulk density from All samples included percent fines as a single factor (R^2 = 0.93, p-value < 0.001; Figure 5); organic carbon explained less of the variation in bulk density

Table 2 Means, medians, and standard deviations of sediments grouped by regional dataset for bulk density; D50 (mm), which is the median particle size; fines; and organic carbon.

	ρ_{dry} (g cm^{-3})			D50 (mm)			P_{fine}			P_{OC}		
	mean	median	SD	mean	median	SD	mean	median	SD	mean	median	SD
All	0.690	0.515	0.34	0.038	0.009	0.08	78.89	93.99	28.62	1.38	1.31	0.90
Bay	0.576	0.481	0.28	0.030	0.009	0.06	86.68	96.07	23.44	1.35	1.27	1.01
Delta	0.892	0.917	0.34	0.054	0.010	0.10	64.92	77.99	32.00	1.42	1.42	0.68

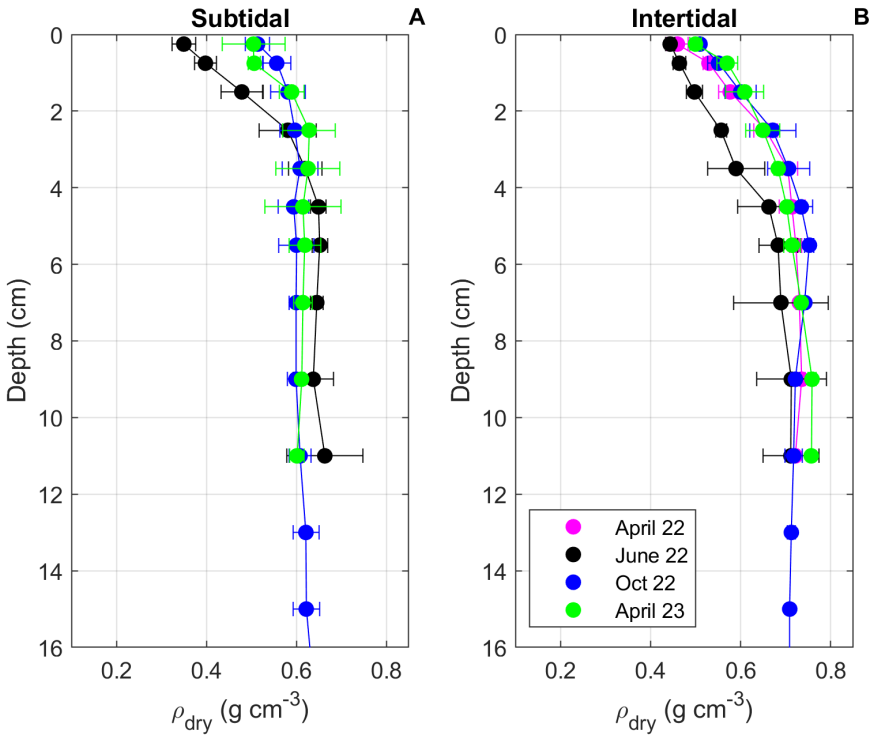

Figure 4 Averages and standard deviations of bulk density with depth (centimeters below sediment bed surface) collected during different months from the shallows of northern San Pablo Bay. (**A**) subtidal shallows (**B**) intertidal shallows.

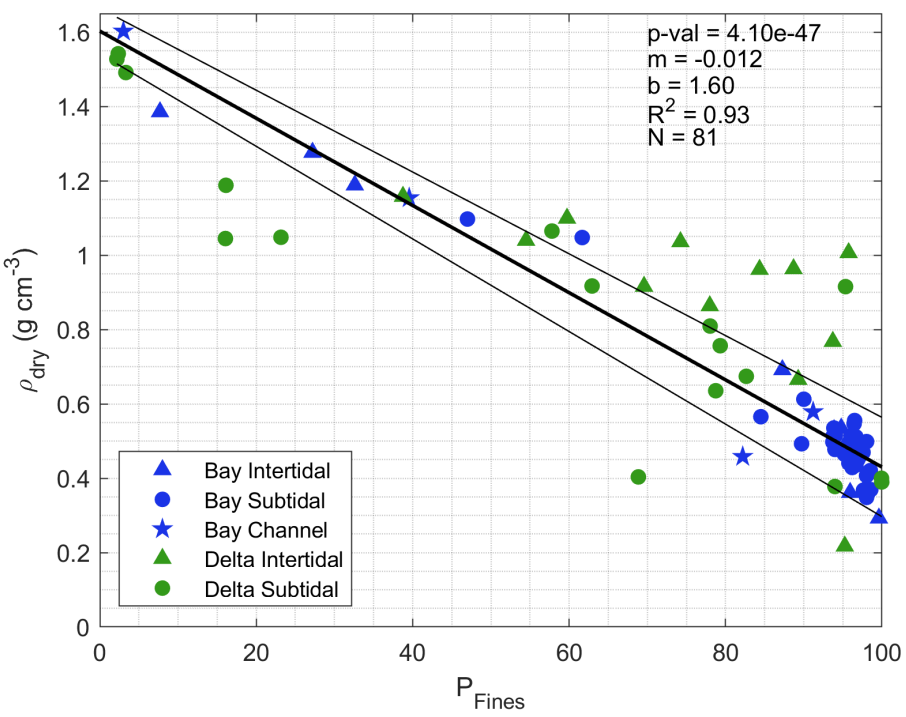

Figure 5 A linear regression model shows percent fines explaining 93% of the variation in bulk density for all sampled sites. The *green* sites are from the Delta; *blue* sites are from the bay. The *thick black line* indicates the regression line, and the *thin black lines* are the 95% confidence intervals.

(R^2 = 0.70). When fines and organic carbon were both used in a multiple regression against bulk density, the adjusted coefficient of determination decreased by ~1% (p-value << 0.001). We examined the potential relationship between fines and organic carbon and found correlation coefficients of 0.73 and 0.77 for the bay and the Delta, respectively.

A comparison between the Bay and Delta models reveals that fines explain 36% more of the variation in bulk density for Bay samples than for Delta samples (Figure 6; Table 3). Organic carbon also explains 36% more of bulk density variability for Bay samples than Delta samples (Figure 6; Table 3). The slopes of the bulk density models for the Bay samples and All samples are not significantly different. However, the slope of the bulk density model for the Delta samples is significantly different from the other two models (Figure 6; Table 3). Although, the difference between the Delta samples and All samples model only becomes apparent for sediments that are approximately 75% fines or more (Figure 6B). Despite the Bay and Delta datasets spanning the same range of bulk density and fines values, the Bay dataset has many data points concentrated in this region of high fines (>75%). There are also 28.2% more Bay samples than Delta samples.

Bulk Density Model Comparison

Among the various models we compared, our All samples bulk density model (Table 3, row 1) and the GF–F model both had the lowest RMSE (0.15) (Figure 7). The GF–F model for sediments from the estuary is:

$$\rho_{dry} = -59495 + 59496 * exp^{\left(\frac{-mud\ content}{5.08e+06}\right)} \quad \text{Eq 8}$$

Although the model is nominally nonlinear, the best fit exponent is so small that it is essentially linear (Figure 7B). These two models performed better than the Mulder model (RMSE: 0.18) followed by the van Rijn model (RMSE: 0.21), then the EFWS–F model (RMSE: 0.24).

Environmental Factors

We also examined the influence of the various environmental factors across the three different datasets: Bay samples, Delta samples, and All samples. Most of the factors examined did not explain the variation in the residuals from our bulk density model (Table 4). However, there were two factors that were significant for the

https://doi.org/10.15447/sfews.2025v23iss4art6

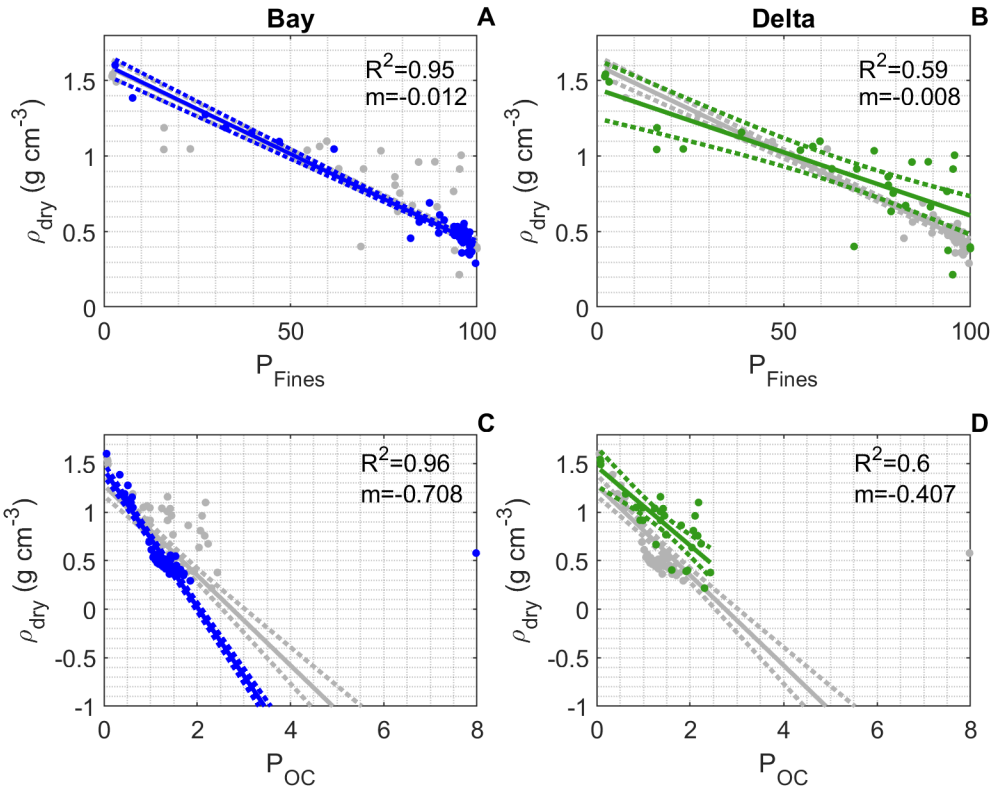

Figure 6 Data and regression lines (*solid line*) for the Bay samples (*blue*), Delta samples (*green*) and All samples combined (*gray*) are shown along with the 95% confidence intervals (*dashed lines*). Plots (**A**) and (**B**) show bulk density vs. fines; plots (**C**) and (**D**) show bulk density vs. total organic content.

Table 3 Regression analysis results for bulk density vs. fines, bulk density vs. organic carbon, and bulk density vs. fines and organic carbon for each dataset: All samples, Bay samples only, and Delta samples only. *P*-values are not shown in this table since all were less than 10^{-6}.

		m	m SE	x2	x2 SE	b	b SE	R^2	Adjusted R^2	RMSE	*N*
ρ_{dry} vs. P_{fines}	All	−0.012	0.0004	—	—	1.60	0.0306	0.93	0.93	0.093	81
	Bay	−0.012	0.0004	—	—	1.61	0.0342	0.95	0.95	0.064	52
	Delta	−0.008	0.0013	—	—	1.45	0.0949	0.60	0.59	0.223	29
ρ_{dry} vs. P_{OC}	All	−0.464	0.0340	—	—	1.28	0.0558	0.71	0.70	0.273	81
	Bay	−0.708	0.0193	—	—	1.44	0.0324	0.97	0.96	0.139	52
	Delta	−0.407	0.0616	—	—	1.47	0.0968	0.62	0.60	0.221	29
ρ_{dry} vs. P_{fines} & P_{OC}	All	−0.012	0.0004	0.004	0.0135	1.60	0.0326	0.92	0.92	0.0987	81
	Bay	−0.009	0.0003	−0.225	0.0075	1.62	0.0272	0.98	0.98	0.0507	52
	Delta	−0.005	0.0020	−0.218	0.0937	1.51	0.0913	0.68	0.65	0.202	29

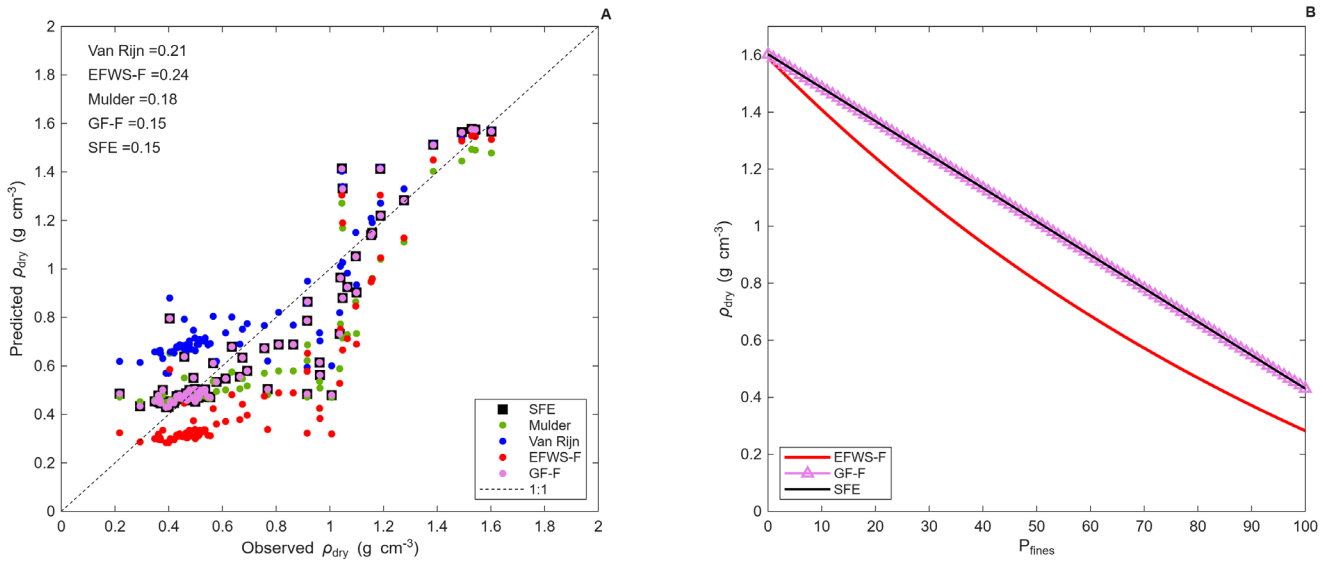

Figure 7 (**A**) Predicted bulk density values plotted against the observed bulk density for each model, with the RMSE from each model shown. (**B**) The regression lines for both Flemming models and our model. Our model for the San Francisco Estuary is labeled as SFE in both figures.

Table 4 Table of results from Kruskal–Wallis tests applied to model residuals for different environmental parameters, broken down by All samples, Bay samples, and Delta samples. For each environmental parameter, group 0 consists of samples where the environmental parameter question is not true, and group 1 consists of samples where it is true. Significant results *(P* < 0.05) are shown in **bold**.

Environmental Factors	Sites	*P*-value	Group 0: N	Group 1: N	Higher BD?	Group 0: Mean rank	Group 1: Mean rank
Energetic?	All	0.277	42	39	calm	43.7	38.1
	Bay	**0.020**	**22**	**30**	**energetic**	**20.8**	**30.7**
	Delta	0.346	20	9	calm	16	12.8
Wavy?	All	0.062	51	30	wavy	37.3	47.4
	Bay	**0.040**	**29**	**23**	**wavy**	**22.6**	**31.3**
	Delta	0.610	22	7	wavy	14.5	16.4
Intertidal?	**All**	**0.018**	**59**	**22**	**inter**	**37.2**	**51.1**
	Bay	0.330	42	10	sub	27.5	22.3
	Delta	**0.021**	**17**	**12**	**inter**	**11.9**	**19.3**
Drought? (DSCI > 100?)	All	0.532	44	37	drought	39.5	42.8
	Bay	0.188	35	17	no drought	28.4	22.5
	Delta	**0.043**	**9**	**20**	**drought**	**10.2**	**17.2**
Saline? (>2 PPT)	**All**	**0.037**	**31**	**50**	**fresh**	**47.9**	**36.7**
	Bay	NA	NA	NA	NA	NA	NA
	Delta	NA	NA	NA	NA	NA	NA

https://doi.org/10.15447/sfews.2025v23iss4art6

All samples dataset, two significant factors for the Delta dataset, and two significant factors for the Bay dataset. For two of the factors, the case associated with higher bulk density was the same across all three datasets: dry season (not shown), and wavy (Table 4). However, these effects were often not significant ($P > 0.05$).

The factors that explained residuals for the Bay samples included waviness and energy, where both wavier and more energetic sites were associated with higher bulk densities. For the Delta samples, tidal regime and DSCI significantly explained the residuals; intertidal sites and drought conditions were both associated with higher bulk densities. When the All samples dataset was examined, we found that fresh (<2 ppt) environments were associated with higher bulk densities, as were intertidal sites. There were not sufficient sample numbers in the saline category (>2 ppt) for the Delta sites and in the fresh category (<2 ppt) for the bay sites, so we could not evaluate those two groups separately. When analyzing the All samples dataset, the saline and fresh categories were very similar to bay sites vs. Delta sites. Therefore, as a check, we examined samples by region (Bay samples vs. Delta samples) to confirm there was not a regional effect driving the significance of the salinity category. Delta sites were associated with higher bulk densities, but this association was not significant (not shown).

Spring or neap and dry or wet seasons were not significant for any of the datasets and are not included in Table 4.

DISCUSSION

Sample Properties and Bulk Density Model

Most of the sediments in our dataset are fines, which are largely representative of the estuary sediments overall. However, some areas within the estuary contain coarser sediment (Barnard et al. 2013). The range of fines in the samples was large; however, most samples were at the finer end of the range (median: 94%, mean: 79%), which might have skewed the model. Additional sampling of regions with coarser sediments may further improve the relationship that we present between bulk density and percent fines. Additional sampling in the Delta would also help to confirm or refute the divergence between the Delta and Bay models for finer sediments. For a sample comprised of 100% fines (where the two models were most divergent), the predicted bulk density is approximately 31% higher for the Delta than for the bay. The Delta dataset had fewer data points than the bay and likely under-represented the diverse water bodies within the Delta.

The slope of the regression line for the Delta model differs from that for the Bay model and All samples combined model (Table 3); however, visual inspection of the regression lines shows that predicted bulk density differed only for sediments with fines >75%. There is more variability in the residuals among the Delta sites, which likely results from the uniqueness of those sites, where external forcings can be more variable than for most bay sites. Middle River, which is a relatively low-energy tidal channel for most of the year—especially during drier years—has coarser sediments with lower-than-predicted bulk density. Finer samples with the greatest residuals were from Little Holland Tract and a few from Liberty Island, which tended to have higher-than-predicted bulk densities. Both sites are former subsided agriculture tracts in which tidal exchange has been restored; their high bulk densities may be a result of compaction during prior agricultural use. Altogether, the varied environments and histories of the different Delta sites might explain why particle size explains only 59% of the variability in bulk density for these samples.

Typically, as in our data, organic carbon is positively correlated with fines (Thomson–Becker and Luoma 1985; Amos et al. 1988; Stephens et al. 1992; Rashid and Reinson 1979; Parker 1982) and is inversely related to bulk density (Amos et al. 1988; Callaway et al. 2012). However, in our data, these correlations (fines and organic carbon; organic carbon and bulk density) were not as strong as the one between fines and bulk density. We attribute this to the low organic carbon content of our samples. Although the range of organic

carbon reached 7.98%, the second highest sample had only 2.32%. The relationships we present are specific to subtidal sites and mudflats. Marsh sediments tend to have higher amounts of organic matter than bay sediments (Lesen 2006; Callaway et al. 2012; Morris et al. 2016). In addition, models of bulk density based on organic content have been developed for tidal wetlands both locally (Callaway et al. 2012), and across many different regions (Morris et al. 2016).

Comparison of Models

The bulk density models from the literature that we compared to our model were developed using sediments from other parts of the world. The nonlinear Flemming (GF–F) model, which performed as well as our (linear) model, required local data to determine the coefficients, unlike the EFWS–F model, which used the same equation form but had coefficients (which were quite different) based on samples from the East Frisian Wadden Sea. This result suggests that these models are regionally dependent and not universally applicable. The use of a model from a specific region might only provide a rough estimate at best when applied to a different system.

The van Rijn model was the only one we considered that incorporated organic matter, and it predicted sediment bulk density with less accuracy than all but one of the models, likely because of the low amounts of organics present in our samples. Particle size appears to be the best predictor of bulk density for sediments from the estuary based on results from this study. However, regions or habitats such as marshes, which have higher amounts of organic matter, may need to incorporate organic content in predictive bulk density models. The influence of other factors known to affect bulk density likely varies from region to region, which is why these models work best when developed for local systems.

Environmental Factors

The environmental factors we chose are associated with sediment transport to some extent, and may influence bed properties. However, we did not identify a factor that significantly explained the residuals of our bulk density models consistently across the three datasets tested.

Waves and Energy

Waves can mobilize sediment from the bed. Egan et al. (2020) observed this in South San Francisco Bay where waves eroded the "fluff" layer of the bed after a period of strong waves, leaving behind a less erodible, more compact sediment bed. Our data demonstrated this phenomenon (waviness leading to higher bulk densities) via the wavy category effect across all datasets (significant only for Bay samples). The energetic category for the bay also supports this idea of strong waves and currents leaving behind a more compact sediment bed. This was not the case for the Delta samples, which had higher bulk densities associated with low energy conditions. The Delta is immediately downstream of the Sacramento and San Joaquin rivers, which are important sources of sediment for the Delta (McKee et al. 2013). High flow events in the Delta likely lead to new deposition of sediment, which gradually consolidates over time during low-flow periods. In addition, high flow may disturb the bed, leading to lower bulk densities.

Spring–Neap Tidal Cycle

Spring tides produce stronger currents and extreme low tides, which increase wave-bed interaction, equating to greater transport and mobilization of sediment. We expected to see spring tides associated with higher bulk densities; however, this effect was not significant for any of the datasets. More transport and mobilization of sediment also creates the potential for more deposition, which might explain the non-significant findings. In San Pablo Bay, the sediment bed was more erodible during spring tides than neap tides, had higher bed stress, and increased sediment resuspension, implying lower bulk density (Allen et al. 2019).

Tidal Regime

Previous work in South Bay showed that bulk density in general is highest at intertidal flats, decreases in shallow subtidal areas, and is lowest

https://doi.org/10.15447/sfews.2025v23iss4art6

in channels (Jones and Jaffe 2013). In our study, intertidal sites were associated with higher bulk densities and significantly explained the model's residuals for All samples and Delta samples. This result might be attributed to the effects exposure has on intertidal sediment, decreasing water content, which in turn increases the bulk density (Anderson and Howell 1984) and resistance to erosion (Amos and Mosher 1985; Amos et al. 1988). However, the effects of exposure on bulk density can be limited for various reasons (e.g., evaporation and precipitation). A study conducted on sediments in a system with mixed semi-diurnal tides found the exposure of intertidal sediments to affect the surface erodibility of sediment but not bulk density, because only a thin layer of sediment dries out during exposure, while bulk density was measured over 1 cm (Amos et al. 1988). This could be one reason why the KW test of our Bay dataset residuals with tidal regime was not significant and did not associate the intertidal with higher bulk density. Overall, the relationship between exposure and bulk density is complex, with contradicting evidence suggesting that additional factors affect this relationship. One argument for intertidal sediments to have lower bulk densities is the tendency of shallower waters in the San Francisco Bay to have higher concentrations of sediment (MacVean and Lacy 2014; Allen et al. 2019) and thus likely to experience more deposition. In addition, shallow mudflats are often closer to sources of fine sediment (i.e., tributaries).

Dry and Wet Seasons and Drought

Bulk density can vary over short time-scales, which might explain why factors that vary over longer time-scales such as dry/wet season did not significantly influence residuals. However, we observed higher bulk densities associated with the dry season for all sites combined (not shown; $p = 0.115$). The wet season is characterized by calm periods broken up by episodic storms that bring rainfall and strong winds, which may lead to the build-up of freshly deposited sediment that has a lower bulk density. In contrast, the dry season is characterized by strong diurnal winds. Winter storms increase the sediment flux from the Delta and other tributaries, which increases the amount of fines (Thomson–Becker and Luoma 1985), and this is associated with the build-up of sediment on intertidal flats in South Bay (Monroe et al. 1992). During droughts, there is diminished flow carrying sediment, which might allow already deposited sediment to be compacted, and might explain why drought conditions were associated with higher bulk density in the Delta and significantly explained the model residuals.

CONCLUSION

An examination of samples collected throughout San Francisco Bay and the Sacramento–San Joaquin Delta shows that percent fines predict bulk density with high accuracy ($R^2 = 0.93$). The model we present is appropriate for the estuary, although the Bay-specific or Delta-specific models also accurately predicted bulk densities. Sediment samples from this study were mostly comprised of mud, had low organic contents, and typically were collected from shallow regions. In systems that are primarily comprised of coarse or organic rich sediment, we would expect that the relationship between percent fines and bulk density may differ. We found a slightly significant difference between bulk density models for the Bay samples and the Delta samples. We also found that the Delta samples had a slightly higher average bulk density and lower fines content than the Bay samples, though neither parameter was significant. The Delta is a large and complex region within the estuary, and we had fewer samples from the Delta than from the bay. Additional samples could help better characterize the relationship between sediment properties for the Delta and help determine whether two different models are necessary for the estuary.

We compared our bulk density model to four models from the literature, which were developed using sediments from other regions. Results suggest that a local model will provide more accurate bulk density predictions than one developed using sediments from a different region.

The model we present here could help improve both sediment transport models and sediment

budgets by providing more accurate bulk density estimates. In addition, the data we present here increase the spatial resolution of measured bulk density for the estuary for use in sediment-transport models and could potentially support planning of beneficial reuse projects.

We assessed the influence of other environmental and hydrographic factors on bulk density and concluded that percent fines–a proxy for particle size–as a single factor was the best predictor. No single environmental parameter significantly explained the residuals of the model for All samples or for the Bay samples and the Delta samples separately. This finding is not surprising given that some of the factors tested are expected to vary in strength between bay and the Delta and, thus, will affect the bay and the Delta differently.

ACKNOWLEDGEMENTS

We thank the USGS Priority Ecosystem Program for San Francisco Bay and the Delta as well as the USGS Coastal and Marine Hazards and Resources Program for funding this project. We express gratitude for Angela Tan and the PCMSC Sediment Lab staff for their careful lab analysis and management of so many samples. We would also like to thank the technicians and boat operators at PCMSC's Marine Facility (MarFac) who made sample collection possible. Thanks to Jenny Thomas and two anonymous reviewers for commenting on a previous draft. Any use of trade, product, or firm names in this paper is for descriptive purposes only and does not imply endorsement by the US government.

DATA ACCESSIBILITY STATEMENT

All data are publicly available; all datasets are cited in Table 1 and included in the references section.

REFERENCES

Akyuz FA. 2017. Drought Severity and Coverage Index. [accessed 2025 Sep 26]. Available from: *https://droughtmonitor.unl.edu/About/AbouttheData/DSCI.aspx*

Allen RM, Lacy JR, Stacey MT, Variano EA. 2019. Seasonal, spring-neap, and tidal variation in cohesive sediment transport parameters in estuarine shallows. J Geophys Res—Oceans. [accessed 2025 Sep 26];124:7265–7284. *https://doi.org/10.1029/2018JC014825*

Allen RM, Lacy JR, Stevens AW. 2021. Cohesive sediment modeling in a shallow estuary: model and environmental implications of sediment parameter variation. J Geophys Res—Oceans. [accessed 2025 Sep 26];126:e2021JC017219. *https://doi.org/10.1029/2021JC017219*

Alonso AC, Maren DS van, Elias EPL, Holthuijsen SJ, Wang ZB. 2021. The contribution of sand and mud to infilling of tidal basins in response to a closure dam. Mar Geol. [accessed 2025 Sep 26];439:106544. *https://doi.org/10.1016/j.margeo.2021.106544*

Amos CL, Mosher DC. 1985. Erosion and deposition of fine-grained sediments from the Bay of Fundy. Sedimentology. [accessed 2025 Sep 26];32:815–832. *https://doi.org/10.1111/j.1365-3091.1985.tb00735.x*

Amos CL, Van Wagoner NA, Daborn GR. 1988. The influence of subaerial exposure on the bulk properties of fine-grained intertidal sediment from Minas Basin, Bay of Fundy. Estuarine Coast Shelf Sci. [accessed 2025 Sep 26];27:1–13. *https://doi.org/10.1016/0272-7714(88)90028-5*

Anderson FE, Howell BA. 1984. Dewatering of an unvegetated muddy tidal flat during exposure—desiccation or drainage? Estuaries. [accessed 2025 Sep 26];7:225–232. *https://doi.org/10.2307/1352142*

Avnimelech Y, Ritvo G, Meijer LE, Kochba M. 2001. Water content, organic carbon and dry bulk density in flooded sediments. Aquac Eng. [accessed 2025 Sep 26];25:25–33. *https://doi.org/10.1016/S0144-8609(01)00068-1*

Barnard PL, Foxgrover AC, Elias EPL, Erikson LH, Hein JR, McGann M, Mizell K, Rosenbauer RJ, Swarzenski PW, Takesue RK et al. 2013. Integration of bed characteristics, geochemical tracers, current measurements, and numerical modeling for assessing the provenance of beach sand in the San Francisco Bay Coastal System. Mar Geol. [accessed 2025 Sep 26];345:181–206. *https://doi.org/10.1016/j.margeo.2013.08.007*

Brand A, Lacy JR, Hsu K, Hoover D, Gladding S, Stacey MT. 2010. Wind-enhanced resuspension in the shallow waters of South San Francisco Bay: mechanisms and potential implications for cohesive sediment transport. J Geophys Res—Oceans. [accessed 2025 Sep 26];115(C11):024. *https://doi.org/10.1029/2010JC006172*

Brew DS, Williams PB. 2010. Predicting the impact of large-scale tidal wetland restoration on morphodynamics and habitat evolution in South San Francisco Bay, California. J Coast Res. [accessed 2025 Sep 26];26:912–924. *https://doi.org/10.2112/08-1174.1*

Callaway JC, Borgnis EL, Turner RE, Milan CS. 2012. Carbon sequestration and sediment accretion in San Francisco Bay Tidal Wetlands. Estuaries Coasts. [accessed 2025 Sep 26];35:1163–1181. *https://doi.org/10.1007/s12237-012-9508-9*

Conomos TJ, Smith RE, Gartner JW. 1985. Environmental setting of San Francisco Bay. Hydrobiologia. [accessed 2025 Sep 26];129:1–12. *https://doi.org/10.1007/BF00048684*

Dadey KA, Janecek T, Klaus A. 1992. Dry-bulk density: its use and determination. Proceedings of the Ocean Drilling Program. Sci Res. [accessed 2025 Sep 26];126:551–554. Available from: *https://www.researchgate.net/publication/237783531_37_DRY-BULK_DENSITY_ITS_USE_AND_DETERMINATION1*

Egan G, Chang G, MacWilliams S, Revelas G, Fringer O, Monismith S. 2020. Cohesive sediment erosion in a combined wave–current boundary layer. J Geophys Res—Oceans. [accessed 2025 Sep 26];126(2). *https://doi.org/10.1029/2020JC016655*

Ezcurra E. 2024. Precision and bias of carbon storage estimations in wetland and mangrove sediments. Sci Adv. [accessed 2025 Sep 26];10(34). *https://doi.org/10.1126/sciadv.adl1079*

Ferreira JCT, Lacy JR, McGill SC, WinklerPrins LT, Nowacki DJ, Stevens AW, Tan AC. 2023a. Hydrodynamic and sediment transport data from Whale's Tail Marsh and adjacent waters in South San Francisco Bay, California 2021-2022. [accessed 2025 Sep 26]. US Geological Survey data release. *https://doi.org/10.5066/P972R6AW*

Ferreira JCT, McGill SC, Tan AC, Lacy JR. 2023b. Grain size, bulk density, and carbon content of sediment collected from Whale's Tail South Marsh and adjacent bay floor, South San Francisco Bay, California, 2021–2022 (verion 2.0, March 2025). [accessed 2025 Sep 26];US Geological Survey data release. *https://doi.org/10.5066/P98BL0XF*

Flemming BW, Delafontaine MT. 2000. Mass physical properties of muddy intertidal sediments: some applications, misapplications and non-applications. Cont Shelf Res. [accessed 2025 Sep 26];20:1179–1197. *https://doi.org/10.1016/S0278-4343(00)00018-2*

Hoaglin DC, Mosteller F, Tukey JW, editors. 1985. Exploring data tables, trends, and shapes. New York: John Wiley & Sons, Inc. 527 p.

Jones CA, Jaffe BE. 2013. Influence of history and environment on the sediment dynamics of intertidal flats. Mar Geol. [accessed 2025 Sep 26]; 345:294–303. *https://doi.org/10.1016/j.margeo.2013.05.011*

Kruskal WH, Wallis WA. 1952. Use of ranks in one-criterion variance analysis. J Am Stat Assoc. [accessed 2025 Sep 26];47:583–621. *https://doi.org/10.2307/2280779*

Lacy JR, Carlson EM, Ferreira JCT. 2016. Wind-wave and sediment-transport time-series data from Liberty Island and Little Holland Tract, Sacramento–San Joaquin Delta, California, 2015–2017. (version 2.0, September 2019). [accessed 2025 Sep 26]. US Geological Survey data release. *https://doi.org/10.5066/F73R0R07*

Lacy JR, Dailey ET, Carlson EM. 2018. Bed sediment properties in Little Holland Tract and Liberty Island, Sacramento–San Joaquin Delta, California, 2014 to 2019. (version 4.0, March 2025). [accessed 2025 Sep 26]. US Geological Survey data release. *https://doi.org/10.5066/F7V1241K*

Lacy JR, Dailey ET, Morgan–King TL. 2023. What controls suspended-sediment concentration and export in flooded agricultural tracts in the Sacramento–San Joaquin Delta? San Franc Estuary Watershed Sci. [accessed 2025 Sep 26];21(1). *https://doi.org/10.15447/sfews.2023v21iss1art4*

Lacy JR, Ferreira JCT, Dailey ET, Dartnell P, Drexler JZ, Allen RM, Stevens AW. 2020a. Sediment transport and aquatic vegetation data from three locations in the Sacramento–San Joaquin Delta, California, 2017 to 2018. [accessed 2025 Sep 26]. US Geological Survey data release. *https://doi.org/10.5066/P9112AIP*

Lacy JR, Foster–Martinez MR, Allen RM, Drexler JZ. 2021. Influence of invasive submerged aquatic vegetation (*E. densa*) on currents and sediment transport in a freshwater tidal system. Water Resour Res. [accessed 2025 Sep 26];57(8):e2020WR028789. *https://doi.org/10.1029/2020WR028789*

Lacy JR, McGill SC, Ferreira JCT, Allen RM, WinklerPrins L, Tan AC. 2020b. Hydrodynamic and sediment transport data from Grizzly Bay and San Pablo Bay, California. Summer 2019. [accessed 2025 Sep 26]. US Geological Survey data release. *https://doi.org/10.5066/P9P7I65U*

Lesen AE. 2006. Sediment organic matter composition and dynamics in San Francisco Bay, California, USA: seasonal variation and interactions between water column chlorophyll and the benthos. Estuarine Coast Shelf Sci. [accessed 2025 Sep 26];66:501–512. *https://doi.org/10.1016/j.ecss.2005.10.003*

MacVean LJ, Lacy JR. 2014. Interactions between waves, sediment, and turbulence on a shallow estuarine mudflat. J Geophys Res—Oceans. [accessed 2025 Sep 26];119:1534–1553. *https://doi.org/10.1002/2013JC009477*

McGill SC, Lacy JR, Ferreira JCT, Allen RM, WinklerPrins L, Tan AC. 2021. Hydrodynamic and sediment transport data from San Pablo Bay and Grizzly Bay, California, 2020. Version 1.1, March 2025). [accessed 2025 Sep 26]. US Geological Survey data release. *https://doi.org/10.5066/P9N88U5G*

McGill SC, Lacy JR, Ferreira JCT, Nowacki DJ, Stevens AW, Tan AC. 2024. Hydrodynamic and sediment transport data from two marshes and adjacent shallows in Northern San Francisco Bay, California 2022–2023. [accessed 2025 Sep 26]. US Geological Survey data release. *https://doi.org/10.5066/P1XZFGCX*

McGill SC, Lacy JR, Stevens AW, Allen RM, Dartnell P, Thede JC, Tan AC, Hatcher GA. 2025b. Oceanographic and hydrographic monitoring data of a shallow-water placement of dredged sediment in South San Francisco Bay, California, 2023–2025. [accessed 2025 Sep 26]. US Geological Survey data release. *https://doi.org/10.5066/P14D723N*

McGill SC, Lacy JR, Tan AC. 2025. Properties of sediment collected from channels in northern San Francisco Bay, California, 2024. [accessed 2025 Sep 26]. US Geological Survey data release. *https://doi.org/10.5066/P13Y6KYK*

McKee LJ, Lewicki M, Schoellhamer DH, Ganju NK. 2013. Comparison of sediment supply to San Francisco Bay from watersheds draining the Bay Area and the Central Valley of California. Mar Geol. [accessed 2025 Sep 26];345(2013):47–62. *https://doi.org/10.1016/j.margeo.2013.03.003*

McKnight K, Lowe J, Plane E. 2020. Special study on bulk density. [accessed 2025 Sep 26]. Contribution #75. Richmond (CA): San Francisco Estuary Institute–Aquatic Science Center (SFEI–ASC). Available from: *https://www.sfei.org/sites/default/files/biblio_files/SFEI_BulkDensityReport_April30_2020_v2.pdf*

Mcleod E, Chmura GL, Bouillon S, Salm R, Björk M, Duarte cm, Lovelock CE, Schlesinger WH, Silliman BR. 2011. A blueprint for blue carbon: toward an improved understanding of the role of vegetated coastal habitats in sequestering CO_2. Front Ecol Environ. [accessed 2025 Sep 26];9:552–560. *https://doi.org/10.1890/110004*

Monroe MW, Kelly J, Lisowski N. 1992. State of the estuary: a report on conditions and problems in the San Francisco Bay/Sacramento–San Joaquin Delta Estuary. Oakland (CA): San Francisco Estuary Project. 270 p.

Morris JT, Barber DC, Callaway JC, Chambers R, Hagen SC, Hopkinson CS, Johnson BJ, Megonigal P, Neubauer SC, Troxler T, et al. 2016. Contributions of organic and inorganic matter to sediment volume and accretion in tidal wetlands at steady state. Earth's Future. [accessed 2025 Sep 26];4:110–121. *https://doi.org/10.1002/2015EF000334*

Mulder H. 1995. De droge dichtheid als functie van het slibgehalte tbv een sedimentbalans. Ministerie van Verkeer en Waterstaat, Rijkswaterstaat RIKZ Werkdocument RIKZ/OS-95614 x.

[NOAA] National Oceanic and Atmospheric Administration. 2024. [accessed 2025 Sep 26]. NOAA Tides Currents. Richmond, CA - Station ID 9414863. Available from: *https://tidesandcurrents.noaa.gov/stationhome.html?id=9414863*

Parker JG. 1982. Structure and chemistry of sediments in Belfast Lough, a semi-enclosed marine bay. Estuarine Coast Shelf Sci. [accessed 2025 Sep 26];15:373–384. *https://doi.org/10.1016/0272-7714(82)90048-8*

Rashid MA, Reinson GE. 1979. Organic matter in surficial sediments of the Miramichi Estuary, New Brunswick, Canada. Estuarine Coast Mar Sci. [accessed 2025 Sep 26];8:23–36. *https://doi.org/10.1016/0302-3524(79)90103-8*

Schoellhamer DH. 1996. Factors affecting suspended-solids concentrations in South San Francisco Bay, California. J Geophys Res—Oceans. [accessed 2025 Sep 26];101:12087–12095. *https://doi.org/10.1029/96JC00747*

Snyder AG, Lacy JR, Stevens AW, Carlson EM. 2016a. Bathymetric survey and digital elevation model of Little Holland Tract, Sacramento–San Joaquin Delta, California: US Geological Survey Open-File Report 2016–1093. [accessed 2025 Sep 26]. Available from: *https://doi.org/10.3133/ofr20161093*

Snyder AG, Stevens AW, Carlson EM, Lacy JR. 2016b. Digital elevation model of Little Holland Tract, Sacramento–San Joaquin Delta, California, 2015. [accessed 2025 Sep 26]. US Geological Survey data release. *https://doi.org/10.5066/F7RX9954*

Stephens JA, Uncles RJ, Barton ML, Fitzpatrick F. 1992. Bulk properties of intertidal sediments in a muddy, macrotidal estuary. Mar Geol. [accessed 2025 Sep 26];103:445–460. *https://doi.org/10.1016/0025-3227(92)90031-C*

Thomson–Becker EA, Luoma SN. 1985. Temporal fluctuations in grain size, organic materials and iron concentrations in intertidal surface sediment of San Francisco Bay. Hydrobiology. [accessed 2025 Sep 26];129:91–107. *https://doi.org/10.1007/BF00048689*

[USGS] US Geological Survey. 2024. USGS National Water Dashboard. [accessed 2024 Sep 25]. Available from: *https://dashboard.waterdata.usgs.gov/app/nwd/en/*

van Rijn LC, Barth R. 2018. Settling and consolidation of soft mud–sand layers. J Waterway Port Coast Ocean Eng. [accessed 2025 Sep 26];145(1). *https://doi.org/10.1061/(ASCE)WW.1943-5460.0000483*

Walters RA, Cheng RT, Conomos TJ. 1985. Time scales of circulation and mixing processes of San Francisco Bay waters. Hydrobiologia. [accessed 2025 Sep 26];129:13–36. *https://doi.org/10.1007/BF00048685*

Weisebron LE, Steiner N, Morys C, Ysebaert T, Bouma TJ. 2021. Sediment bulk density effects on benthic macrofauna burrowing and bioturbation behavior. Front Mar Sci. [accessed 2025 Sep 26];8. *https://doi.org/10.3389/fmars.2021.707785*

Wentworth CK. 1922. A scale of grade and class terms for clastic sediments. J Geol. [accessed 2025 Nov 3];30(5):377-392. Chicago (IL): The University of Chicago Press. Available from: *https://www.jstor.org/stable/30063207?seq=1*

Wright SA, Schoellhamer DH. 2004. Trends in the sediment yield of the Sacramento River, California, 1957–2001. San Franc Estuary Watershed Sci. [accessed 2025 Sep 26];2(2). *https://doi.org/10.15447/sfews.2004v2iss2art2*